Electrochemical Fabrication of Silver Dendrites as an Excellent Platform for Surface Enhanced Raman Scattering Application

Chao Li[1], Ruihui Dai[2], Xiaojia Wu[3], Ruifang Qi[2] and Jingjun Ma[3,*]

[1] College of Sciences, Agricultural University of Hebei, Baoding 071001, P.R. China
[2] Department of Basic Courses, Agricultural University of Hebei, Huanghua 061100, P.R. China
[3] College of Science and Technology, Agricultural University of Hebei, Huanghua 061100, P.R. China
[*]E-mail: jingjunma_hebeiag@foxmail.com

The synthesis of silver dendritic framework can be achieved by scattering graphene oxide (GO) into the solution of $AgNO_3$. This convenient electrochemical method with single stage involved was issued in the work. A clear-cut dendritic framework of the silver object generated by such synthesis was shown by means of scanning electron microscopy. What is more, the observation of X-ray Diffraction revealed the cubic phase of the silver. GO's existence was indicated in silver dendrites by way of UV-Vis spectroscopy, in which GO went through electrochemical reduction as the silver was deposited. With the existence of GO and $AgNO_3$, this research assessed the SERS approach's improvement as well as analysis capacity demonstrated in the measurement of canola oil and α-tocopherol. In addition, the work researched into the practicability of adopting such SERS approach to analysing canola oil' oxidation. The results revealed that SERS was highly sensitive in the analysis of dilute canola oil and α-tocopherol, and that in a mixture it was possible to analyse such constituents above at the same time.

1. INTRODUCTION

Synthesizing precious metal nanostructures with the set shape has been tremendously appealing over nearly ten years since a material's morphological form could influence the traits as well as practical uses in a great way [1, 2]. Nanostructures in fractal and dendritic forms stood out from diverse forms of such structures, appealing to many researchers on account of the special catalytic, optical as well as electrical property [3, 4]. For instance, researchers have explored dendrites of silver's possible practical uses, including biochemical sensor [5, 6], catalysis [7], superhydrophobic surface [8] as well as surface-enhanced Raman scattering (SERS) detection [9]. To synthesize the

silver in dendritic forms, there were several approaches like template approach [10], non-template straight growth [11], electro-deposition [12], sono-electrochemical approach [13], photo-reduction [14] and microwave approach [15]. Over the past few years, featuring the adoption of Si, Al, Cu and Zn as sacrifice materials, galvanic replacement was issued with its capacity to synthesize silver dendrites [16-20]. In galvanic replacement, where electrochemical reaction occurs, one metal (generally known as a sacrifice) is oxidized when another one's ions are more elevated in reduction potential. As soon as they meet in solution, the sacrificial metal would go through oxidization as well as dissolution. Meanwhile, the reduction of another metal's ions would occur then they would be adhered to the appearance of the sacrificial metal by plating. Because such an approach features great productivity without complex processes at the same time, it has been appealing to many researchers. There is no denying that diverse issued researches explored synthesizing silver dendrites by means of galvanic replacement. However, scarce study has been conducted for preparing potential objects for synthesizing silver dendrites.

In the molecular scope, Raman spectroscopy works through vibration for measuring the chemical "tracks" of the to-be-analysed material with no damage caused at fast speed [21-23]. It has diverse applications, including the characterization of bulk lipids' chemical structure as well as the discrimination of various cooking oils and fats [24], the detection of fake oil [25, 26], and the determination of free fatty acid content [27]. In addition, ramen spectroscopy was applied for the observation of lipid oxidization in bulk oils. In oxidization process, the vibration of chemical bonds change, resulting from oxidation-related molecular alterations. By means of FT-Raman spectroscopy, the chemical alterations are observed to occur in lipid oxidation in six plant oils [27, 28]. What is more, this method was applied to research the natural oxidation of a few unsaturated fatty acid methyl esters [29]. Made according to their performance on the analysis lipid oxidization such as peroxide value (PV), anisidine value (AV), conjugated diene, and hexanal [28], the comparison between Raman spectroscopy and other traditional measuring methods reveals that the former one if more favourable in that it could offer facts about the chemical structure of lipid as well as its oxidized form. [28]. Moreover, another comparison has been made between Raman spectroscopy and gas chromatography. The results show that it is extremely simple to prepare material with the former method, while the latter approach needs much work to be done to process the samples in advance. Meanwhile the traditional Raman spectroscopy has its disadvantages like being limited to analysing bulk oil due to the basically weak signals. This could be compensated by the nanostructure of noble metals like gold, through which the signal could be greatly boosted by charge shift and electromagnetism [22]. SERS, namely surface enhanced Raman spectroscopy has experienced widespread exploration since it is characterized by high sensitivity of molecule. Meanwhile this method has gained diverse application in biological and chemical sensing through transducing signals.

Through target molecules' adsorption and concentration and SERS signal's magnification, grapheme is regarded to be potential to be applied to SERS sensing. Until now there have been several researches indicating that graphene oxide having gone through functionalization behaved outstandingly in SERS sensing [30]. Thus, it should be worthwhile to research into the compound of silver dendrites and grapheme with functions of them together embodied. It is also worth exploring the composite's strengthening effects exerted on SERS sensing. In this research, Ag dendrites' synthesis is

issued by means of electrochemical generation approach. The SERS performance of Ag dendrites processed like that is afterwards researched to observe the process of canola oil oxidation.

2. EXPERIMENTS

2.1. Chemicals

The powder of graphene oxide (GO) could be purchased in JCNANO, INC. (China). Sigma-Aldrich was a place to commercially obtain 3-hydroxytyramine hydrochloride (DA), L-Ascorbic acid (AA, 99%), poly (sodium 4-styrene-sulfonate) (PSS, Mw = 70000), silver nitrate (AgNO3) and Uric acid (UA, 99%). The rest materials needed were pure in an analytical sense and could be applied as they were purchased. Delta Technologies (USA) introduced glasses covered by ITO with a R_{est} of 10 $\pm$ 2 Ω. Besides, the buffer solution (PBS) was generated by putting KH2PO4 into K2HPO4 to make a mixture with appropriate pH achieved through adjustment. It is worth noting that all the experiments were conducted with the Milli-Q water (18.2 MΩcm) used.

2.2. Electrodeposition of silver nanostructures

Being scattered into 10 ml of water, 4 mg of GO experiences one hour's ultrasonic treatment. Then the GO dispersed water and 50 mM of $AgNO_3$ solution made a short time before were put together to make a mixture, which was used as electro-deposition solutions, with diverse proportions of them. By means of a triple- electrode approach as well as cyclic voltammetry (CHI430A, CH Instruments, Ausin, TX, USA), Ag went through electro-deposition on the electrodes of ITO. As for the study, there was also reference electrode, embodied by Ag/AgCl with KCl (3M). Besides, there was assistant electrode, with the use of a wire of platinum. The cyclic voltammetry scan was adjusted to range from 0 to -1.6 V, with the scan rate 20 mV/s. This was followed by rinsing ITO for two times with Milli-Q water. Since there were different proportions of $AgNO_3$ to GO, namely, 1:12, 1:8 and 1:4, there were correspondingly three diverse products: GO/Ag-1, GO/Ag-2 and MWCNT-GO/Ag-3, which were gained through the above approach.

2.3. Characterization

Raman spectroscopy was conducted through Raman Microprobe (Renishaw RM1000) with the experiment's subjects being receiving a laser illumination of 514 nm at ambient temperature. As for the optical measurements, this study adopted the UV-Vis spectrophotometer (Halo RB-10, Dynamic Pty Ltd, AU), with the wavelength's range of 190 to 800 nm. In addition, to achieve the characterization of the morphological state of the materials prepared ithrough the above mentioned approach, the stufy adopted the field emission scanning electron microscopy (FeSEM, ZEISS SUPRA 40VP, Germany). Meanwhile, to achieve the characterization of these materials' structures, Cu K radiation has been utilized.

2.4. SERS analysis

To measure the oxidation of oil, canola oil (1 mL) sealed in vials (25 mL) went through incubation in the oven with the temperature adjusted to be 55 °C. To make them analysed by SERS, 1 vial should leave the oven to be cooled to ambient temperature every twenty-four hours. This was followed by canola oil's dilution and combination with hexane. The analysis was compared with another treatment. In order to observe the oxidization of lipid, conjugated dienes went through spectrophotometrical measurement every 24 hours. By means of spectrophotometer, the absorbance of conjugated diene was 234 nm. This was conducted by dissolving canola oil samples that had been weighted into isooctane at the proper dilution factor. The experiment's results referred to conjugated dienes' millimoles in canola oil (1 kg), with an absorptivity of 26,000 for conjugated linoleic acid (Chan & Levett, 1977). Presented as the mean and standard deviation, the whole set of experiments were conducted in three samples.

3. RESULTS AND DISCUSSION

As an effective approach, cyclic voltammetry was applied to produce electro-deposition equipment. Figure 1 indicated the primary cyclic voltammetric monitor of ITO electrode in the solution of $AgNO_3$ dispersed with GO. The CV profile of $GO/AgNO_3$ at -0.40 V revealed a slight reduction crest. Such a crest represented that the metallic Ag was achieved after Ag+ was reduced [31]. Negative surface charges due to the GO which could attract positively charged silver ions and become the nucleation sites for Ag nanoparticles. The electric field gradient near the Ag nanoparticles formed on the entangled surface is much larger than that of the electrode surface. Hence, this electric field directs the movement of silver ions to generate the dendritic structure.
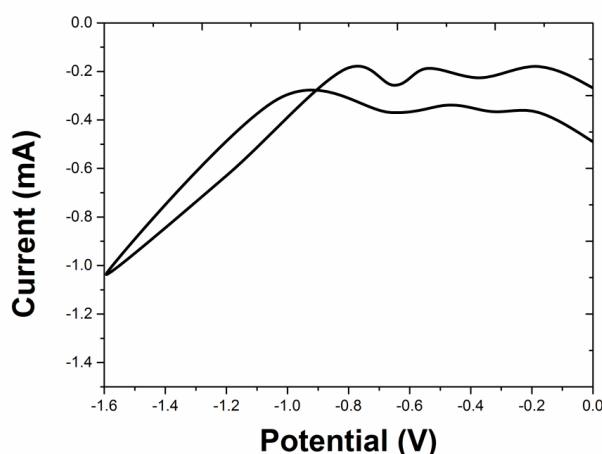

Figure 1. The cyclic voltammograms of the ITO electrodes in the mixed solutions of $GO/AgNO_3$.

After the appearance of Ag dendrites, the diffusion-limited-aggregation (DLA) model could well illustrate the fractal growth [32, 33]. The DLA regime involves cluster growth by the adhesion of a particle to a seed on contact and growing surface after the reduction. In the present study, after the initial reduction of Ag ions, the surface region of ITO is depleted of Ag ions, synchronously increasing the double layer. In addition, without a supporting electrolyte the potential should immediately drop. The Ag ions from the bulk solution migrate to the tip of preformed baby Ag dendrites due to the effect of higher electric field gradient [34]. Therefore, the Ag ions continuously attach to the preformed Ag nanoparticles and become the stem part of the dendrites. In addition, the diffusion of Ag ions plays a dominant role in the formation of Ag branches and elongates the existing stems [35].

Shaped in this way, the Ag with dendritic structure then shifted to the water pre-treated by deionization after its removal from the electrode. This was followed by the measurement of Ag dispersion in the above solution through UV-Vis spectroscopy, as was shown in Figure 2A. It could been seen in the figure that at 231 nm GO was at its highest. This could be due to the $\pi \rightarrow \pi^*$ transition of aromatic C=C bonds in GO [36]. On the other hand, when it comes to the GO/Ag having been electro-synthesized, the crest of 231 nm changes to 257 nm. Meanwhile, there is a decline of crest intensity. Such changes shows the reduction of GO in the nanocomposite [37]. In addition, Ag formation could be evidenced by the single broad absorption peak with a maximum at 380 nm due to its surface plasmon resonance (SPR) absorption. Such observation also contributes to the fact that Ag has been formed. The crest intensity, together with the spot where the crest occurs on Ag SPR band depends on nanomaterials' form and size to a large extent. As is shown in the figure, the crests are not symmetric, which indicates the formation of supermolecule [31]. In order to state that GO is reduced, the study adopts Raman spectroscopy. Figure 2B reveals that through the Raman spectra, for GO the crest was shown to be at 1600 cm^{-1}, while for GO/Ag the crest was at 1350 cm^{-1}. Due to the diamondoid (D) bands, the crest appears when the wavenumber is lower. On the contrary, the crest appears when the wavenumber is higher, because of the graphite (G) bands. The increase of D to G (I_D/I_G)'s peak intensity ratio from 0.89 to 1.07 indicates reduction brings about the generation of graphite with plenty of defects [38].
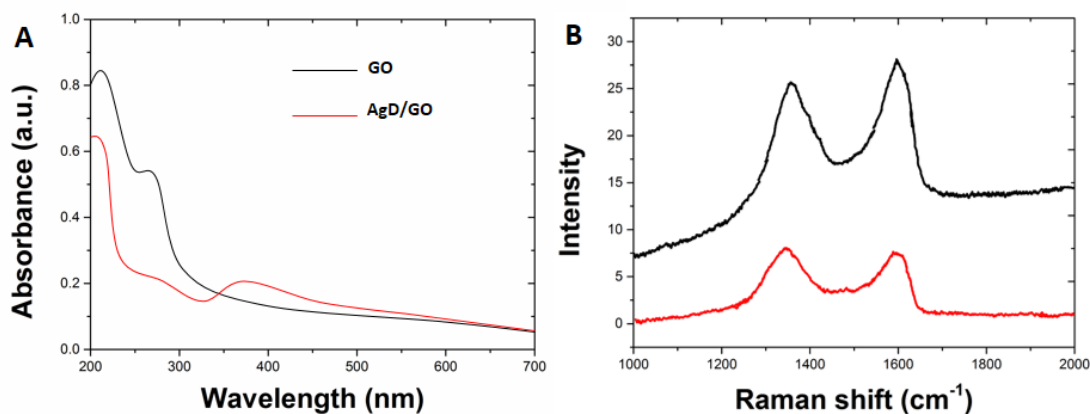

Figure 2. (A) UV-Vis absorption spectra of GO and GO/Ag aqueous dispersion; (B) Raman spectra of GO and GO/Ag.

Figure 3 indicated that GO/Ag with diverse Ag proportion went through measurement of XRD, with data shown in the figure. It could be obviously noted in Figure 3A that a typical crest was in accordance with the GO powder in its crude state at 11.1°. Such a crest coincided with GO's (001) plane and an inter-planar space of 0.82 nm [39]. On the contrary, there was no such crest occurring in the rest of GO/Ag generated above treated by XRD. Such a comparison reveals GO has been reduced in electro-deposition. Besides, XRD reveals Ag's cubic form (JCPDS file No. 04-0783) existing in GO/Ag. The Ag cubic form's (111) plane accounts for the peak with a high intensity at 36.50°, which indicates Ag deposition facilitates this plane in trial conditions. As the rate of Ag rises, intensity of these peaks at 42.67°, 62.92°, 75.90° and 79.83° is raised step by step. Those peaks are respectively linked with the (200), (220), (311) and (222) plane of Ag fcc (face-centered-cube) crystal.
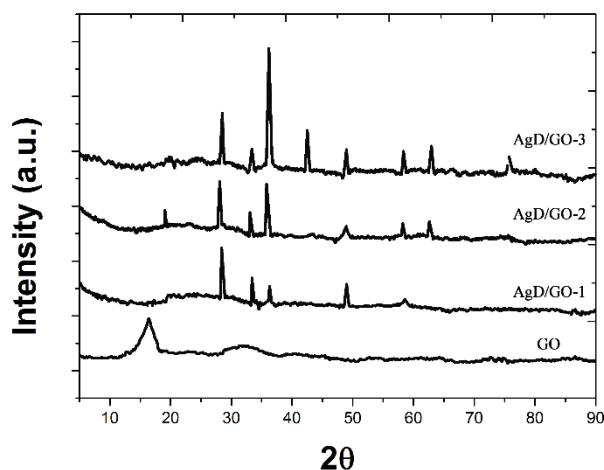

Figure 3. XRD patterns of GO/Ag with different Ag proportion: GO powderand GO/Ag coated ITO.
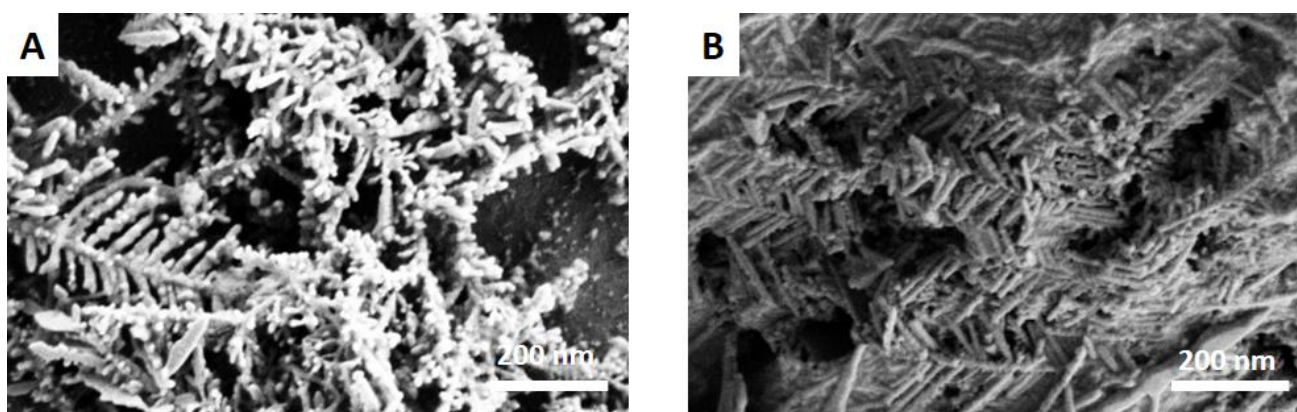

Figure 4. SEM images of (A) Ag dendrites and (B) GO/Ag composite.

SEM monitored the morphological state of the Ag dendrites (AgD) under above synthesis treatment and GO/Ag composite. Figure 4 characterises AgD and GO/Ag composite in the form of SEM images with equivalent amplification. Figure 4A showed that AgD shaped through galvanic replacement is made up of a trunk and plenty of surrounding branches. The branches do not meet with

each other, with an angle of 54° with the trunk. Figure 4B indicated that GO exerts nearly no influence on the generation of AgD in the GO/Ag, where there is not clear morphological alteration monitored, even with extremely magnified SEM pictures. Nevertheless, as for the GO/Ag, there are carpets of GO, carpeting or linking the branches and trunks of single dendrite.

To study the enhancement effect of GO/Ag on diluted α-tocopherol and canola oil, we compared the SERS spectra with the normal Raman spectra under the same condition. As shown in Figure 5A, the normal Raman spectrum of 5% α-tocopherol (without GO/Ag) only showed weak signals. Nevertheless, when GO/Ag base was applied, the spectrum got boosted and the crest intensity was elevated. GO/Ag base, together with α-tocopherol contributed to the occurrence of the crests. The crests from the base majorly lay in the remaining NO_3^- when the base was prepared. The obvious crest at about $1075 \ cm^{-1}$ could be regarded to be interior standard crest to show the related amount of the analysed materials on the silver appearance during their competition for binding. As the molecules of the analysed materials accumulate on the Ag appearance, the NO_3^- crest decline. The extraction of silver base could be conducted on the spectra if necessary. The main crests indicated in the traditional Raman spectrum in perfectly pure α-tocopherol all appear on SERS spectrum. The band at $2875 \ cm^{-1}$ stood for the CH stretching. The bands around 1447 indicated CH_3 deformations. Meanwhile, CH_2 deformation was shown through $1342 \ cm^{-1}$. The bands at around 597 and $492 \ cm^{-1}$ was the prerequisite to observe ring deformations. Such facts indicated GO/Ag's ability of strengtheningα-tocopherol's Raman dispersion.
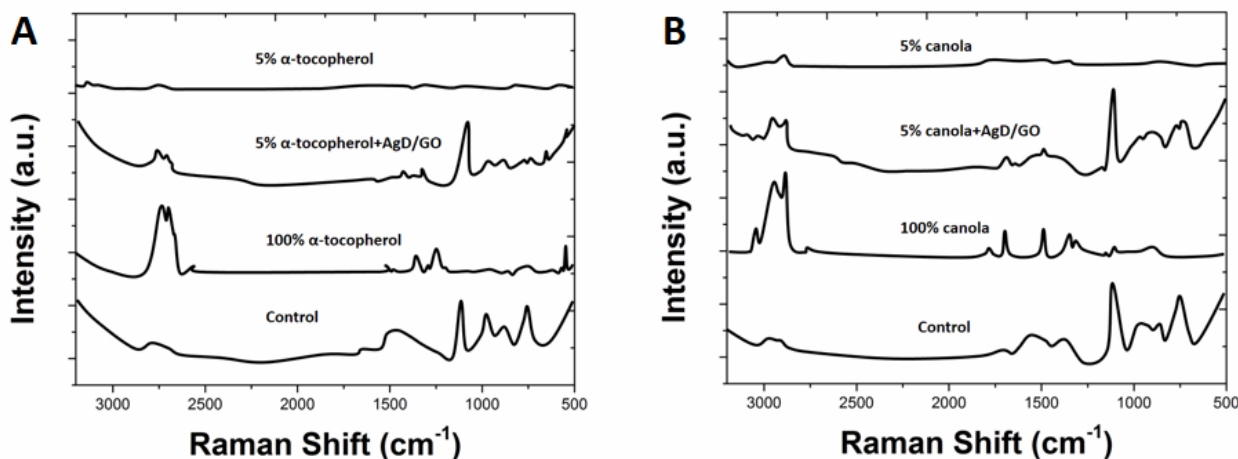

Figure 5. SERS and normal Raman spectra of (A) α-tocopherol and (B) canola oil.

AgD's capacity of strengthening canola oil's Raman dispersion was also indicated. Figure 5B indicated nearly the same strengthening effect with the Ag base adopted in 5% canola oil, with crest intensity as the assessing standard. Such obvious effect was seen with its comparison with the traditional Raman spectrum in the same circumstance. The band standing for the CH stretch was observed at $2848 \ cm^{-1}$. The band standing for the C=C stretch was noted at $1665 \ cm^{-1}$. The band at around $1451 \ cm^{-1}$ stands for the transformation of CH_3 and CH_2. It was intriguing that through the optical monitor of canola oil, a crest of $1618 \ cm^{-1}$ occurs specially through SERS method. However,

when it comes to the traditional Raman one and the Ag containing one, this did not happen. Besides, such crest appeared exclusively in roughly half of the chosen materials like the one mentioned above. Why such crest happened could not be explained. One possible explanation was that one of lipid molecules' special frameworks got strengthened because they interacted randomly with silver appearance. Due to the straight deposition of samples on AgD's appearance, there was a disarrayed organization of their molecules on the appearance, thus leading to randomly displayed crest. Another possibility is that this peak may be from the enhancement of another compound that presented in a trace amount in the canola oil [40, 41]. Hence we can't see it in the normal Raman spectra and the compound may not uniformly present on the Ag surface due to the trace amount. Further study is needed to elucidate the origin of this interesting peak. Nevertheless, this data indicated the improved sensitivity of the lipid measurement using the GO/Ag.

The facts and statistics above revealed the diverse sensitivity and various SERS signature shown between canola oil and α-tocopherol, which indicated the potential to detect canola oil and α-tocopherol using Ag dendrites at the same time. SERS spectra of 5% canola oil, 5% α-tocopherol, and 5% of their mixture (10% α-tocopherol in canola oil) were shown in Figure 6. Obviously, canola oil signals and α-tocopherol signals were both included in the SERS spectra of the last sample. It was pretty easy to see the dash line, which referred to α-tocopherol's Raman bands. But it did not have a desirable effect because of the pre-existence of tocopherol used as antioxidant in the purchased canola oil. Meanwhile, it was impossible for above SERS approach to conduct the detection of it. The most important reason is that prior to SERS's working, canola oil need to be diluted. After dilution, canola oil is reduced to 5%. Correspondingly, the concentration of tocopherol normally contained reduces to just 0.05%. However, the statistics indicates it was possible for the detection of antioxidant and oil at the same time. Meanwhile, to equip SERS signals with more sensitivity, further researches are also necessary for the enhancement of SERS substrate, as well as the optimization of conditions concerning instruments and preparing section.
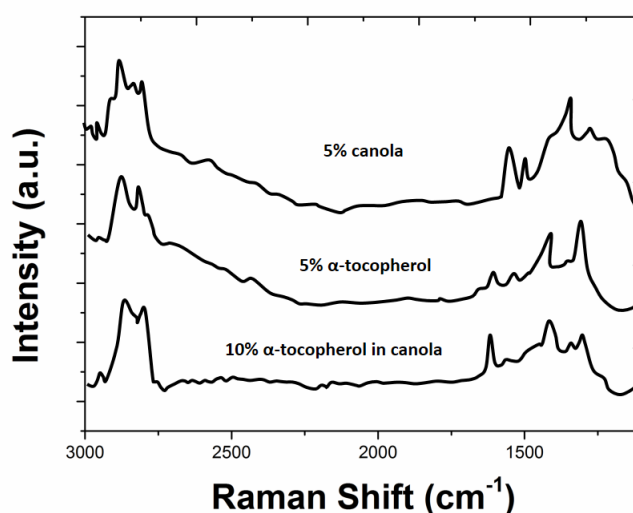

Figure 6. SERS spectra of 5% canola oil, 5% α-tocopherol, and 10% mixture of α-tocopherol in canola oil (with concentration of 5% through dilution).

The Raman spectra of the oil were measured with oil of different densities. Even if perfectly pure oil was adopted, the spectra shown on day 0 did not vary from that monitored on day 30 (Figure 7), with the re sults indicating that the statistics of the spectra obtained in this way were almost the same. On day 5, with the analysis of PCA plot, an obvious shift of SERS spectra could be observed. Meanwhile, the data cluster observed on this day could be clearly differentiated with those of day 0. This figure showed that the whole set of crest intensity tended to decline. It is worth mentioning that the crest intensity experienced a sharp decline on day 7. Since the crest intensity on day 7 did not differ very much from that of day 30, it could be indicated that intensity declined much slower during this period. Probably because of no reaction product, key lipid crests declined from 2947 to 2852, 1663, and 1457 cm^{-1}. Limit of detection (LOD) and limit of quantification (LOQ) values were calculated based on the formula reported [42]. Nevertheless, along with the above decline, the Ag background crest also experienced a drop. Through comparison, the crest decline of Ag background was much sharper than that of lipid. For instance, NO_3^- crest dropped to 1073 cm^{-1}. Through previous discussion, to a certain extent, NO_3^- crest acted as an indicative factor for other elements of silver dendrites. To state it in detail, as the NO_3^- crest declined, it was suggested that the number of silver dendrites' molecules rose, which would be regarded as oxidized resultants, like alcohols, saturated aldehydes, α, β-unsaturated aldehydes and epoxy compounds. Prior to them, there were already a group of resultants through oxidization. When the latter produced oxidization resultants' molecules existing on the silver dendrites' appearance were ultimately most, which could be boosted by the Ag, the whole group of crest intensity would decline, deceived by such an illusion. The oil was treated by dilution to 0.1% on day 30, in order to confirm the proposal.
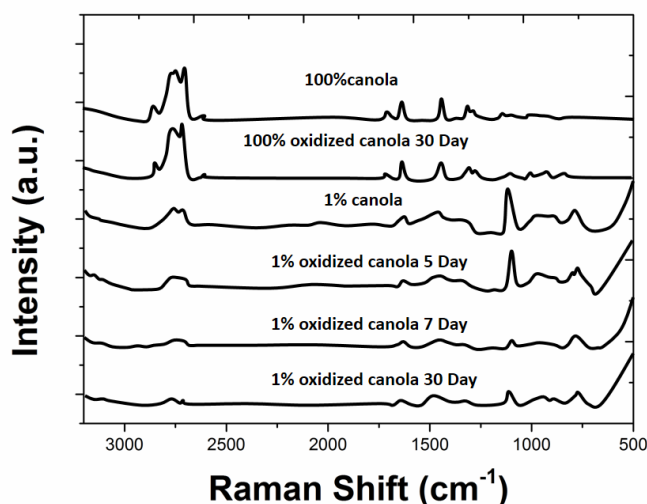

Figure 7. Normal Raman spectra of commercial canola oil (100%) on day 0 and after 30 days of incubation.

4. CONCLUSIONS

In this study, an electrochemical deposition approach with single stage involved for the synthesis of AgD/GO composite was illustrated. Raman spectroscopy, together with UV-Vis observed

the reduction of GO occurring in electro-deposition. The cubic Ag shaped in the experiment has dendritic structure has been characterized by SEM as well as XRD. by means of SERS, Ag dendrites' strengthening capacity exerted for analysing α-tocopherol and canola oil was assessed. With the experiments conducted on both compounds, SERS signals were more sensitive than traditional Raman signals. But the results also show that there were not so much elements and scope for to better the strengthening effects.

References

1. A. Tao, S. Habas and P. Yang, *Small*, 4 (2008) 310.
2. C. Yin, G. Lai, L. Fu, H. Zhang and A. Yu, *Electroanalysis*, 26 (2014) 409.
3. S. Wang, L. Xu, Y. Wen, H. Du, S. Wang and X. Zhang, *Nanoscale*, 5 (2013) 4284.
4. L. Fu, T. Tamanna, W. Hu and A. Yu, *Chemical Papers*, 68 (2014) 1283.
5. T. You, O. Niwa, M. Tomita and S. Hirono, *Anal. Chem.*, 75 (2003) 2080.
6. L. Fu, G. Lai, B. Jia and A. Yu, *Electrocatalysis*, 6 (2015) 72.
7. J. Huang, S. Vongehr, S. Tang, H. Lu, J. Shen and X. Meng, *Langmuir*, 25 (2009) 11890.
8. X. Zhang, F. Shi, J. Niu, Y. Jiang and Z. Wang, *Journal of Materials Chemistry*, 18 (2008) 621.
9. Q. Zhang, Y. Chen, Z. Guo, H. Liu, D. Wang and X. Huang, *ACS Applied Materials & Interfaces*, 5 (2013) 10633.
10. J. Zhang, F. Huang and Z. Lin, *Nanoscale*, 2 (2010) 18.
11. W. Ren, S. Guo, S. Dong and E. Wang, *J Phys Chem C*, 115 (2011) 10315.
12. L. Fu, G. Lai, P.J. Mahon, J. Wang, D. Zhu, B. Jia, F. Malherbe and A. Yu, *RSC Advances*, 4 (2014) 39645.
13. S. Tang, X. Meng, H. Lu and S. Zhu, *Mater. Chem. Phys.*, 116 (2009) 464.
14. Y. Zhou, S.H. Yu, C.Y. Wang, X.G. Li, Y.R. Zhu and Z.Y. Chen, *Adv. Mater.*, 11 (1999) 850.
15. M. Noroozi, A. Zakaria, M. Moksin, Z.A. Wahab and A. Abedini, *International Journal of Molecular Sciences*, 13 (2012) 8086.
16. W. Ye, Y. Chen, F. Zhou, C. Wang and Y. Li, *Journal of Materials Chemistry*, 22 (2012) 18327.
17. A. Avizienis, C. Martin-Olmos, H. Sillin, M. Aono, J. Gimzewski and A. Stieg, *Crystal Growth & Design*, 13 (2013) 465.
18. I. Shao and L. Gignac, *ECS Transactions*, 41 (2012) 9.
19. J. Dong, H. Zheng, X. Yan, Y. Sun and Z. Zhang, *Applied Physics Letters*, 100 (2012) 051112.
20. S. Xie, X. Zhang, S. Yang, M. Paau, D. Xiao and M. Choi, *RSC Advances*, 2 (2012) 4627.
21. S. Harvey, M. Vucelick, R. Lee and B. Wright, *Forensic Science International*, 125 (2002) 12.
22. C. Haynes, A. Mcfarland and R. Duyne, *Anal. Chem.*, 77 (2005) 338 A.
23. C. Porter, C. Pouton, J. Cuine and W. Charman, *Advanced Drug Delivery Reviews*, 60 (2008) 673.
24. H. Yang, J. Irudayaraj and M. Paradkar, *Food Chemistry*, 93 (2005) 25.
25. V. Baeten, J. Fernández Pierna, P. Dardenne, M. Meurens, D. García-González and R. Aparicio-Ruiz, *Journal of Agricultural and Food Chemistry*, 53 (2005) 6201.
26. H. Yang and J. Irudayaraj, *Journal of the American Oil Chemists' Society*, 78 (2001) 889.
27. B. Muik, B. Lendl, A. Molina-Dí and J. Ayora-Cañada, *Anal. Chim. Acta.*, 487 (2003) 211.
28. B. Muik, B. Lendl, A. Molina-Díaz and M. Ayora-Cañada, *Chemistry and Physics of Lipids*, 134 (2005) 173.
29. J. Agbenyega, M. Claybourn and G. Ellis, *Spectrochimica Acta Part A: Molecular Spectroscopy*, 47 (1991) 1375.
30. L. Fu, D. Zhu and A. Yu, *Spectrochimica Acta Part A: Molecular and Biomolecular Spectroscopy*, 149 (2015) 396.
31. S. Kaniyankandy, J. Nuwad, C. Thinaharan, G. Dey and C. Pillai, *Nanotechnology*, 18 (2007)

125610.

32. T. Witten, Jr. and L. Sander, *Physical Review Letters*, 47 (1981) 1400.
33. E. Ben-Jacob and P. Garik, *Nature*, 343 (1990) 523.
34. N. Abbasi, P. Shahbazi and A. Kiani, *Journal of Materials Chemistry A*, 1 (2013) 9966.
35. H. Xun, G. Wang, Y. Wang, W. Zhu and X. Shen, *Chinese Journal of Chemical Physics*, 23 (2010) 596.
36. J. Paredes, S. Villar-Rodil, A. Martínez-Alonso and J. Tascón, *Langmuir*, 24 (2008) 10560.
37. Y. Zhou, Q. Bao, L.A.L. Tang, Y. Zhong and K. Loh, *Chemistry of Materials*, 21 (2009) 2950.
38. J. Yang, J. Zheng, H. Zhai and L. Yang, *Cryst Res Technol*, 44 (2009) 87.
39. T. Nakajima, A. Mabuchi and R. Hagiwara, *Carbon*, 26 (1988) 357.
40. S. Velioglu, H. Temiz, E. Ercioglu, H. Velioglu, A. Topcu and I. Boyaci, *Food Chemistry*, 221 (2017) 87.
41. W. Chua, P. Chapman and G. Stachowiak, *Journal of the American Oil Chemists' Society*, 89 (2012) 1793.
42. M. Gondal, Z. Seddigi, M. Nasr and B. Gondal, *J. Hazard. Mater.*, 175 (2010) 726.